Computational and Structural Biotechnology Journal 20 (2022) 5672–5679

COMPUTATIONAL ANDSTRUCTURAL BIOTECHNOLOGY JOURNAL

journal homepage: www.elsevier.com/locate/csbj

Big dynorphin is a neuroprotector scaffold against amyloid β-peptide aggregation and cell toxicity

Lucía Gallego-Villarejo [a,1], Cecilia Wallin [b,1], Sylwia Król [b,1], Jennifer Enrich-Bengoa [a,1], Albert Suades [a,b], Marcel Aguilella-Arzo [c], María José Gomara [d], Isabel Haro [d], Sebastian Wärmlander [b], Francisco J. Muñoz [e], Astrid Gräslund [b], Alex Perálvarez-Marín [a,*]

[a] Unit of Biophysics Dept of Biochemistry and Molecular Biology, Institute of Neurosciences, Universitat Autònoma de Barcelona, Facultat de Medicina, 08193 Cerdanyola del Vallés, Catalonia, Spain
[b] Department of Biochemistry and Biophysics, Stockholm University, Stockholm, Sweden
[c] Laboratory of Molecular Biophysics, Department of Physics, University Jaume I, 12071 Castellón, Spain
[d] Unitat de Síntesis i Aplicacions Biomèdiques de Pèptids, Institut de Química Avançada de Catalunya, IQAC-CSIC, Jordi Girona, 18-26, 08034 Barcelona, Catalonia, Spain
[e] Laboratory of Molecular Physiology, Faculty of Health and Life Sciences, Universitat Pompeu Fabra, Barcelona, Catalonia, Spain

ARTICLE INFO

Article history:
Received 21 July 2022
Received in revised form 9 October 2022
Accepted 9 October 2022
Available online 14 October 2022

Keywords:
Alzheimer's disease
Amyloid β-peptide
Dynorphins
Peptide therapy
Biophysics

ABSTRACT

Amyloid β-peptide (Aβ) misfolding into β-sheet structures triggers neurotoxicity inducing Alzheimer's disease (AD). Molecules able to reduce or to impair Aβ aggregation are highly relevant as possible AD treatments since they should protect against Aβ neurotoxicity. We have studied the effects of the interaction of dynorphins, a family of opioid neuropeptides, with $A\beta_{40}$ the most abundant species of Aβ. Biophysical measurements indicate that $A\beta_{40}$ interacts with Big Dynorphin (BigDyn), lowering the amount of hydrophobic aggregates, and slowing down the aggregation kinetics. As expected, we found that BigDyn protects against $A\beta_{40}$ aggregates when studied in human neuroblastoma cells by cell survival assays. The cross-interaction between BigDyn and $A\beta_{40}$ provides insight into the mechanism of amyloid pathophysiology and may open up new therapy possibilities.

© 2022 Published by Elsevier B.V. on behalf of Research Network of Computational and Structural Biotechnology. This is an open access article under the CC BY-NC-ND license (http://creativecommons.org/licenses/by-nc-nd/4.0/).

1. Introduction

Alzheimer's disease (AD) is caused by the misfolding of the amyloid-β peptide (Aβ) into β-sheets forming neurotoxic oligomers and fibrils [1,2]. Therapies directed to inhibit Aβ aggregation and/or to disassembly the aggregated forms are one of the main aims in AD research [3,4], but most of them are not succeeding [5]. Promising results using an Aβ-binding antibody have been obtained recently in AD patients showing attenuated clinical decline [6].

AD is a multifactorial disease where Aβ plays a key role but other mechanisms also contribute to AD onset and progression, such as the AD risk factor ApoE4 [7]. In fact, the reasons why Aβ starts to aggregate in the brain parenchyma are unknown. The Aβ variants of 40 and 42 residues ($A\beta_{40}$ and $A\beta_{42}$, respectively) have shown different tendency to aggregate, with $A\beta_{42}$ being the most fibrillogenic isoform, but $A\beta_{40}$ is the most abundant in both healthy and AD patients and both types are present in the senile plaques [8]. Metal chemistry has been shown to be of great importance to understand AD [9,10]. However, it seems that cross-interaction of Aβ with other amyloid and non-amyloid endogenous molecules is opening new ways to develop new diagnostics and therapeutics strategies [11,12].

Dynorphins are prohormone opioid endogenous peptides derived from prodynorphin (PDYN) [13], which are the canonical substrate for kappa-opioid receptors [14]. Prodynorphin is cleaved at positively charged residues motifs by proprotein convertase (PC2) and other enzymes. It is processed into shorter intermediates, such as big dynorphin (BigDyn, 32 residues), which is further processed into dynorphin A (DynA, 17 residues) and dynorphin B (DynB, 13 residues) [13]. Dynorphins are some of the most positively charged peptides found in our body [15] (Table 1), which makes them highly prone to interact with negatively charged molecules, such as the negatively charged polar head groups of phospholipids [16] and also other molecules, e.g. the Aβ (Table 1).

Studies on endogenous opioid systems in AD neuropathology have shown altered μ-, δ-, and κ-opioid receptor binding capabilities [18–20]. Dynorphins, as substrates for these receptors, have

* Corresponding author.
E-mail address: alex.peralvarez@uab.cat (A. Perálvarez-Marín).
[1] Equally contributed.

https://doi.org/10.1016/j.csbj.2022.10.014
2001-0370/© 2022 Published by Elsevier B.V. on behalf of Research Network of Computational and Structural Biotechnology.
This is an open access article under the CC BY-NC-ND license (http://creativecommons.org/licenses/by-nc-nd/4.0/).

Table 1
Peptide physico-chemical properties.

Peptide	Primary sequence	Mol. weight[a]	pI[a]	Charge[a]	GRAVY Index[a]
$A\beta_{40}$	$DAEFR_5HDSGY10EVHHQ_{15}KLVFF_{20}AEDVG_{25}SNKGA_{30}IIGLM_{35}VGGVV_{40}$	4329.8	5.2	−3	0.06
DynA	YGGFL5RRIRP10KLKWD15NQ	2147.5	11.5	+4	−1.26
DynB	YGGFL5RRQFK10VVT	1574.8	11.4	+3	−0.11
BigDyn	$YGGFL_5RRIRP_{10}KLKWD_{15}NQKRY_{20}GGFLR_{25}RQFKV_{30}VT$	3984.7	12.2	+9	−0.98

[a] Analysis performed using Expasy ProtParam tool [17].

been found to be dysregulated in AD, especially DynA [21]. In addition, AD shows elevated levels of PC2, the enzyme processing PDYN into BigDyn, and further into DynA and DynB [21,22]. In the initial stages of AD, it has been shown that Aβ oligomers primarily target synapses [23], where altered PDYN processing may lead to changes in dynorphin levels, such as increased DynA presence. Here, we study the cross-interaction between $A\beta_{40}$ and dynorphins based on the premises that: i) DynA is dysregulated in AD [21], ii) dynorphins and $A\beta_{40}$ share the same location at the brain parenchyma, and iii) potential $A\beta_{40}$-dynorphins interactions could be driven by electrostatics and hydrophobicity.

2. Materials and methods

2.1. Peptide-peptide docking

Dynorphin A, B, and Big dynorphin were modelled in i-Tasser using the DynA 1–13 structure (PDB code 2N2F) [14] and using the secondary structure restraints derived from Hugonin et al. [24]. The structure of choice for $A\beta_{40}$ peptide was PDB code 1BA4 [25]. Peptide-peptide docking was performed in Patchdock [26] and further refined with the Docking2 option in Rosie server [27]. The docking poses were ranked by total score and by interfacial score [28].

2.2. Molecular dynamics simulations and analysis

The big dynorphin- $A\beta_{40}$ peptide-peptide complex was prepared and replicated three times in solution for energy minimization and equilibration in CHARMM-GUI [29], using the CHARMM36m force field [30]. The equilibrated output for each complex was reassembled in CHARMM-GUI to produce a complex containing three BigDyn-$A\beta_{40}$ complexes. As control, a system containing three $A\beta_{40}$ peptides was also prepared. Simulations consisted of 5000 steepest descent minimization steps and six NPT equilibration steps in which the restrictions applied on the protein and membrane are released and the timestep gradually increased from 1 fs to 2 fs. MD simulations contained a Parrinello-Rahman pressure coupling and Particle Mesh Ewald for electrostatics and Nose-Hoover for the temperature coupling, extended during 200 ns and at 310.15 K for the production step. Analysis of the trajectories secondary structure conversions was performed using and in-house Python script on the data output from the Timeline plugin in VMD [31].

2.3. Peptides

Recombinant $A\beta_{40}$ (with the primary sequence of $DAEFR_5HDSGY10EVHHQ_{15}KLVFF_{20}AEDVG_{25}SNKGA_{30}IIGLM_{35}VGGVV_{40}$) and big dynorphin (BigDyn) (primary sequence of $YGGFL_5RRIRP_{10}KLKWD_{15}NQKRY_{20}GGFLR_{25}RQFKV_{30}VT$) were purchased from Alexotech (Umeå, Sweden). Dynorphin A (DynA) and dynorphin B (DynB) were bought from Neosystem Laboratoire (France) with the primary sequences of YGGFL5RRIRP10KLKWD15NQ and YGGFL5RRQFK10VVT, respectively (Table 1). Peptides were also synthesized in-house by solid-phase peptide synthesis (SPPS) as C-terminal carboxamide following a 9-fluorenylmethoxycarbonyl (Fmoc) strategy. NovaSyn® TGR resin (500 mg, 0.2 meq/g) and Fmoc-protected amino acids (Novabiochem, Merck Millipore, Merck KGaA, Darmstad, Germany) were used. Amino acid side chain protection was effected by the following: triphenylmethyl (Trt) for glutamine and asparagine; *tert*-butyl (tBu) for aspartic acid, and tyrosine; 2,2,5,7,8-pentamethyl-chroman-6-sulfonyl (Pmc) for arginine and *tert*-butoxycarbonyl (Boc) for lysine and tryptophan. The coupling reaction was performed by treatment of Fmoc-amino acids (3 eq.) with 2-(1H-7-azabenzotriazole-1-yl)-1,1,3,3-tetramethyluronium hexafluorophosphate methanaminium (3 eq.) (HATU) (Genscript, Piscataway, NJ, USA) and diisopropylethylamine (6 eq.) (DIPEA) (Fluka-Sigma-Aldrich, St. Louis, MO, USA) in dimethylformamide (DMF) (Scharlau, Barcelona, Spain). The Fmoc deprotection step was performed twice with 20 % piperidine (Fluka-Sigma-Aldrich, St. Louis, MO, USA) in DMF for 10 min. The stepwise addition of each residue was assessed by the ninhydrin test and chloranil test for identification of primary and secondary amines, respectively. The peptides were simultaneously side chain deprotected and cleaved from the resin by treatment with a mixture of trifluroacetic acid (TFA) (Scharlau, Barcelona, Spain), triisopropylsilane (TIS) (Fluka-Sigma-Aldrich, St. Louis, MO, USA) and water (TFA/TIS/H2O, 9.5/2.5/2.5, v/v/v) for 3 h with occasional agitation at room temperature. The solvent was removed in vacuum and the crude peptides were precipitated with diethyl ether (Merck, KGaA, Darmstad, Germany). The solids were dissolved in 30 % acetic acid (Panreac, AppliChem GmbH, Darmstadt, Germany) in water and lyophilized.

The crude peptides were purified by semi-preparative HPLC (1260 Infinity, Agilent Technologies, Santa Clara, CA, USA) in an XBridgeTM Prep BEH130 C18 column (5 μm, 10 × 250 mm, Waters, Milford, MA, USA). The purified peptides were characterized by UHPLC on an Acquity UHPLC (Waters, Milford, MA, USA) chromatograph using an Acquity UHPLC BEH C18 reverse-phase column (2.1 × 100 mm, 1.7 μm particle size). Peptide samples were dissolved in a mixture of acetonitrile (Fisher Scientific, Loughborough, UK) and water (1/1, v/v) and analyzed in the UPLC at a flow rate of 0.3 mL/min. Linear gradients of solvent B (20 mM formic acid in acetonitrile) into solvent A (20 mM formic acid in water) over 10 min at 0.3 mL/min were performed for peptide elution. Both a variable wavelength UV detector and an electrospray ionization mass spectrometry (ESI-MS) were connected to the UHPLC for peptide characterization. UV detection was carried out at a wavelength of 220 nm. ESI-MS was performed with a liquid chromatograph–time of flight (LC-TOF) detector, LCT Premier XE (Micromass Waters, Milford, MA, USA). The mass spectra were recorded in positive ion mode in the *m*/*z* 500–2500 range. The purity of the peptides was higher than 95 % by UHPLC.

2.4. Sample preparation

For NMR and ThT kinetics experiments, recombinant non-labeled or uniformly 15 *N*-labeled $A\beta_{40}$ peptides were bought lyophilized from AlexoTech AB (Umeå, Sweden). The lyophilized

peptides were stored at −80 °C until used. High-monomer content samples were prepared by dissolving the $A\beta_{40}$ in 10 mM NaOH, pH 12, at a concentration of 1 $mg{\cdot}ml^{-1}$ and sonicated in an ice-bath for at least three minutes. The peptide concentration was determined by weight or spectrophotometrically by absorbance at 280 nm. Further dilution was done in 10 mM sodium phosphate buffer pH 7.2–7.4. All samples were kept on ice.

All dynorphin peptides were dissolved in Milli-Q water and the concentration was determined by absorbance at 280 nm with an extinction coefficient of 6970 $M^{-1}{\cdot}cm^{-1}$ for DynA and 1280 $M^{-1}{\cdot}cm^{-1}$ for DynB, and 8250 $M^{-1}{\cdot}cm^{-1}$ for Big Dyn.

Aggregated samples for hydrophobicity analysis and cell toxicity measurements were prepared by incubating dynorphins alone or in the presence of $A\beta_{40}$ peptides for 30 h at + 37 °C, representative of a ThT aggregation kinetics end-point (see below). Aggregated mixtures were snap-frozen in liquid nitrogen and kept at −80 °C until further use.

2.5. Thioflavin T aggregation kinetics

Prior to kinetic experiments an extra step with size exclusion chromatography (*SEC*) using a Superdex 75 10/300 GL column (GE Healthcare) was performed for the $A\beta_{40}$ sample to remove any pre-formed aggregates [32]. One $mg{\cdot}ml^{-1}$ $A\beta_{40}$ in 10 mM NaOH or in Gd·HCl (Fig. S3) was injected to the equilibrated *SEC* column and eluted with a flow rate of 0.5 $mL{\cdot}min^{-1}$ in 10 mM sodium phosphate buffer pH 7.4 at room temperature. The collected fractions were immediately moved to ice. The monomeric peak was collected and the peptide concentration was determined spectrophotometrically by absorbance at 280 nm with an extinction coefficient of 1490 $M^{-1}{\cdot}cm^{-1}$. The $A\beta_{40}$ peptides were further diluted in Eppendorf tubes to 12 μM in 10 mM sodium phosphate buffer pH 7.4 and supplemented with 40 μM Thioflavin T (ThT) as an amyloid probe [33,34] and different concentrations of DynA, DynB, and BigDyn peptides. The samples were distributed onto a 96-well plate, 100 μL per well, and fluorescence was measured every second minute with a 440 nm excitation filter and a 480 nm emission filter during quiescent conditions at + 37 °C in a FLUOstar Omega microplate reader (BMG LABTECH, Germany). Four replicates per condition were measured. The ThT fluorescence kinetic traces were analyzed using sigmoidal curve fitting according to Eq.1 [35], allowing the parameters aggregation halftime, τ½, and the maximum growth rate, rmax, to be determined.

$$F(t) = F_0 + \frac{A}{1 + \exp[r_{max}(\tau 1/2) = t]} \quad (1)$$

where F0 is the fluorescence signal intensity baseline, A is the fluorescence intensity amplitude, r_{max} is the maximum growth rate and the aggregation halftime, τ½, corresponds to when the monomeric Aβ peptide population is half depleted.

2.6. NMR spectroscopy

2D NMR 1H-15 N- heteronuclear single quantum coherence (HSQC) spectra were recorded on a 500- or 700 MHz Bruker Avance spectrometers equipped with cryoprobes at +5 °C. The temperature was chosen due to optimal signal intensity and to avoid $A\beta_{40}$ aggregation. Either DynA, DynB, or BigDyn was titrated onto one sample each with 84 μM monomeric 15N-labeled $A\beta_{40}$ peptides in 10 mM sodium phosphate buffer pH 7.4 (90/10 H2O/D2O). The 15N-labeled $A\beta_{40}$ concentration was determined by weight. The 2D NMR HSQC data was processed with the Topspin version 3.2 software and referenced to the 1H signal of trimethylsilylpropanoic acid (TSP). The $A\beta_{40}$ amide crosspeak assignment in the HSQC spectra was known from previously published work [36].

2.7. Reverse phase HPLC

Aggregated peptide mixtures were quenched in 2 % TFA and injected in a Waters 2690 HPLC coupled to a UV detector set to 280 nm. A linear gradient of 25 %-45 % of 0.1 % TFA in acetonitrile was applied for 90 min into a 250x4.6 mm (5 μm) C4 column (Phenomenex) at a flow rate of 0.75 mL/min.

2.8. MTT cell viability assays

Aggregated samples of 25 μM $A\beta_{40}$, 10 μM DynA, 10 μM DynB, 10 μM BigDyn and mixtures of $A\beta_{40}$ with each of the Dynorphins were prepared maintaining the concentrations. SH-SY5Y, a human neuroblastoma cell line, was used in the study. Cells were seeded in 96-well plates at density of 10,000 cells/100 μL/well and incubated at 37 °C for 24 h. An $A\beta_{40}$ dose-concentration curve was performed and 3.75 μM $A\beta_{40}$ was chosen for the experiments since they produced a neurotoxicity response around 40 %. Cells were challenged with the different treatments and the toxicity was evaluated after 24 h of incubation. Then 11 μL of 3-(4,5-dimethylthiazol-2-yl)-2,5-diphenyltetrazolium bromide (MTT) solution were added to each well and incubated for 2 h. The reaction was stopped with DMSO and absorbances were measured at 570 nm and 655 nm. Control cells were assumed as 100 % viability. For statistical analysis one-way Analysis of Variance (ANOVA) was performed and corrected by Bonferroni's multiple comparison test.

3. Results

First, to assess the potential interaction between dynorphins and $A\beta_{40}$ we use computational docking (Fig. 1). The peptide cross-interaction is highly likely due to electrostatics, but other physicochemical parameters are relevant, and taken into account in computational docking algorithms such as Rosie [27]. The global docking is assessed by total score (Fig. 1A), but also by the energy of the actual docking interface, namely interface score (Fig. 1B). DynA and DynB show a total score of −35 and −32 kcal/mol, respectively, while BigDyn docking poses are less convergent, but with a lower average total score of −40 kcal/mol. Taking into account both energy terms, the most balanced docking solution corresponds to BigDyn/$A\beta_{40}$ complex, with total score and interface mean score of −40 kcal/mol and −5 kcal/mol, respectively. Thus, to assess the complex stability, the lowest energy BigDyn/$A\beta_{40}$ complex in both terms of global docking and the actual interface docking region (-5.5 interface score; −45 total score in Fig. 1C) is selected as a representative conformation (Fig. 1D).

To validate the dynorphin-Aβ binding interaction we applied 2D NMR experiments to obtain/reveal residue-specific information. Uniformly ^{15}N-labeled monomeric $A\beta_{40}$ peptides feature a well-resolved 2D NMR HSQC spectrum. Non-labeled DynA, DynB and BigDyn peptides were sequentially titrated upon a ^{15}N-labeled $A\beta_{40}$ peptide sample. Neither the titration of DynA nor DynB showed any specific binding towards the monomeric Aβ peptide, as observed by none-significant signal intensity reduction (data not shown). Titration of BigDyn induced gradual resonance signal attenuations in a concentration-dependent manner (Fig. 2A and Fig. S1). At equimolar BigDyn and Aβ concentrations (Fig. S1) approximately 60 % of the signal intensity had decreased. The loss of signal indicates chemical exchange on the intermediate NMR timescale or potential loss of monomeric peptides into larger structures invisible by solution NMR. Higher concentrations of BigDyn above stoichiometric ratios induced visible precipitation of the sample, arguing for the formation of large BigDyn-$A\beta_{40}$ complexes (Fig. S1). The gradual decrease of signal intensity is uniform and

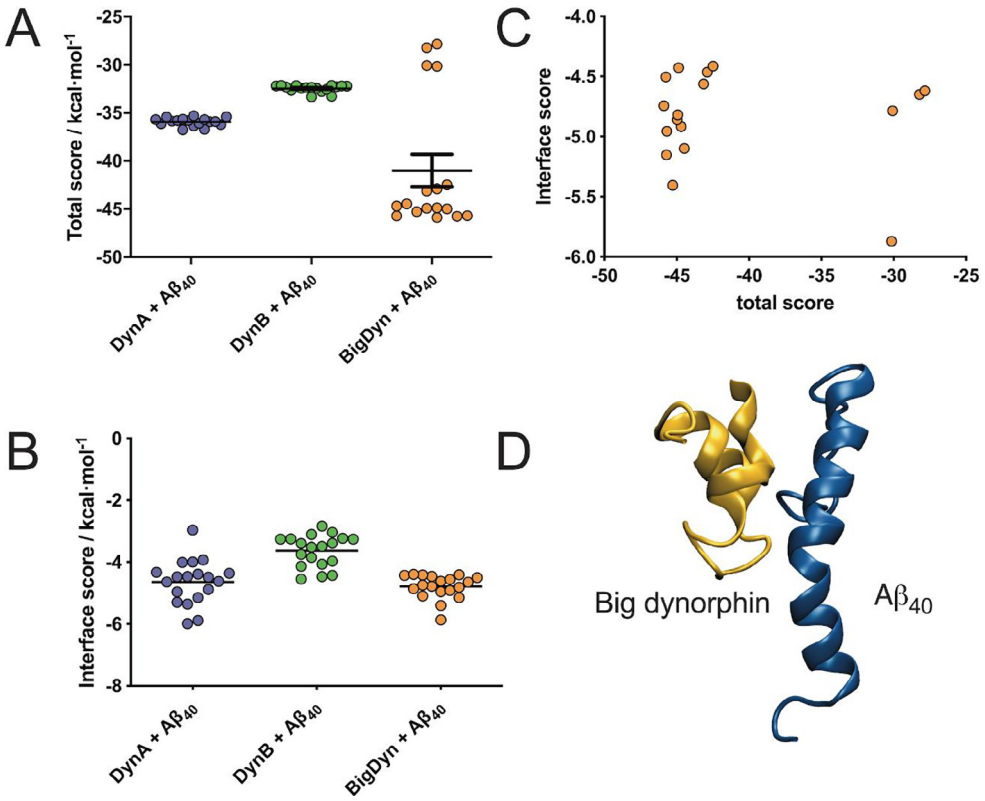

Fig. 1. Peptide-peptide docking. A. Global peptide-peptide docking analysis represented by the total score. B. Local peptide-peptide docking analysis represented by the interface score. C. Cross-correlation between total and interfaces scores to select the most-balanced docking solution (indicated by arrowhead). D. Peptide-peptide docking pose of choice based the ratio between total and interface score.

non-specific over the primary peptide sequence, with slightly larger signal attenuation of the N-terminal part of the Aβ peptide.

To obtain further details of the dynorphin-Aβ_{40} interactions, Thioflavin T (ThT) fluorescence labelling was used to study the aggregation kinetics for Aβ_{40} alone and in the presence of dynorphins (Fig. 2B and Table 2). ThT is a small molecule that becomes highly fluorescent when binding to amyloid material like that formed from the Aβ peptides after suitable incubation [33,34]. It is worth to mention that dynorphins alone did not show any increase of ThT fluorescence intensity after incubation (Fig. S2). DynA incubated with Aβ_{40} increases 0.8-fold the amyloid aggregation level (as shown by the endpoint of ThT fluorescence intensity, Fig. 2B and Table 2). DynB and BigDyn incubated with Aβ_{40} decrease the amyloid aggregation level 1.5-fold and 1.8-fold, respectively. Regarding kinetics, the Aβ_{40} samples incubated with dynorphins show a slower amyloid formation process (as shown by the $\tau_{½}$ parameter, Table 2) with 4.4, 3.9, and 5.6 h for the samples incubated with DynA, DynB, and BigDyn, respectively, as compared to 2.5 h for Aβ_{40} alone under the same conditions. The dynorphin-induced slowing down of the Aβ_{40} amyloid formation is also shown in the aggregation kinetics rate (r_{max} in Table 2) with 1.2, 1.7 and 0.5 h^{-1} for DynA, DynB, and BigDyn, respectively, compared to 3.5 h^{-1} for Aβ_{40} alone. Aβ_{40} is prepared as monomer for the ThT experiments (see Material and Methods section for details), we analyzed the anti-aggregation profile of BigDyn against Aβ_{40} nucleated samples, where oligomers and other high molecular species may be present, still showing a slower amyloid formation process (Fig. S3).

To assess the role of dynorphins on the nature of the aggregates, hydrophobicity analysis by RP-HPLC (Table 1 for peptides theoretical hydropathy GRAVY indexes) of the peptide mixtures was carried out after a 30-hour incubation (Fig. 2C). Aβ_{40} alone shows a characteristic hydrophobic peak, which is absent in the single dynorphin samples. Aβ_{40} with DynA and DynB mixtures show the chromatogram consisting of the combination of individual peptides, but with lower amyloid content. BigDyn alone is not resolved by hydrophobicity, since it does not show any distinctive peak in the RP-HPLC run, arguing for its high solubility [24]. Aβ_{40} + BigDyn mixture shows a series of peaks corresponding to lower hydrophobicity intermediates compared to the distinctive Aβ_{40} peak (dashed line in Fig. 2C).

The biological effect of the Aβ_{40} + dynorphins mixtures was assessed by the MTT cell viability assay in a human neuroblastoma cell line (SH-S5Y5, Fig. 3). In this setup, the dynorphin peptides alone showed similar viability levels compared to the control (10 mM sodium phosphate buffer pH 7.2). When SH-S5Y5 were treated with Aβ_{40} incubated for 30 h, the viability was reduced to 63.4 ± 9.9 %. Viability levels were: 70.7 ± 12.8 % for Aβ_{40} + DynA and 98.5 ± 8.1 % for Aβ_{40} + DynB. In the case of the Aβ_{40} + BigDyn mixture, the viability was significantly increased to 111.4 ± 2.2 % compared to Aβ_{40} alone (Fig. 3), indicating that BigDyn exerts a cellular neuroprotective effect when incubated with Aβ_{40}.

Although NMR experiments did not show a specific region for the interaction between BigDyn and Aβ_{40} (Fig. S1), we took advantage of the computational setup to gain insight into the molecular determinants of the BigDyn/Aβ_{40} complex. Using the docking pose in Fig. 1D we set the computational system to compare an aggregation-prone situation (three Aβ_{40} peptides randomly placed, Fig. 4A) against three Aβ_{40} peptides complexed with BigDyn (Fig. 4B), as a small representation of the potential interaction landscape of the complex. In the computational setup in Fig. 4A, the three Aβ_{40} peptides quickly interact, and the α-helix structure within the 12–32 residues in Aβ_{40} is rapidly lost towards turn-like and β-extended secondary structures. When Aβ_{40} peptides are

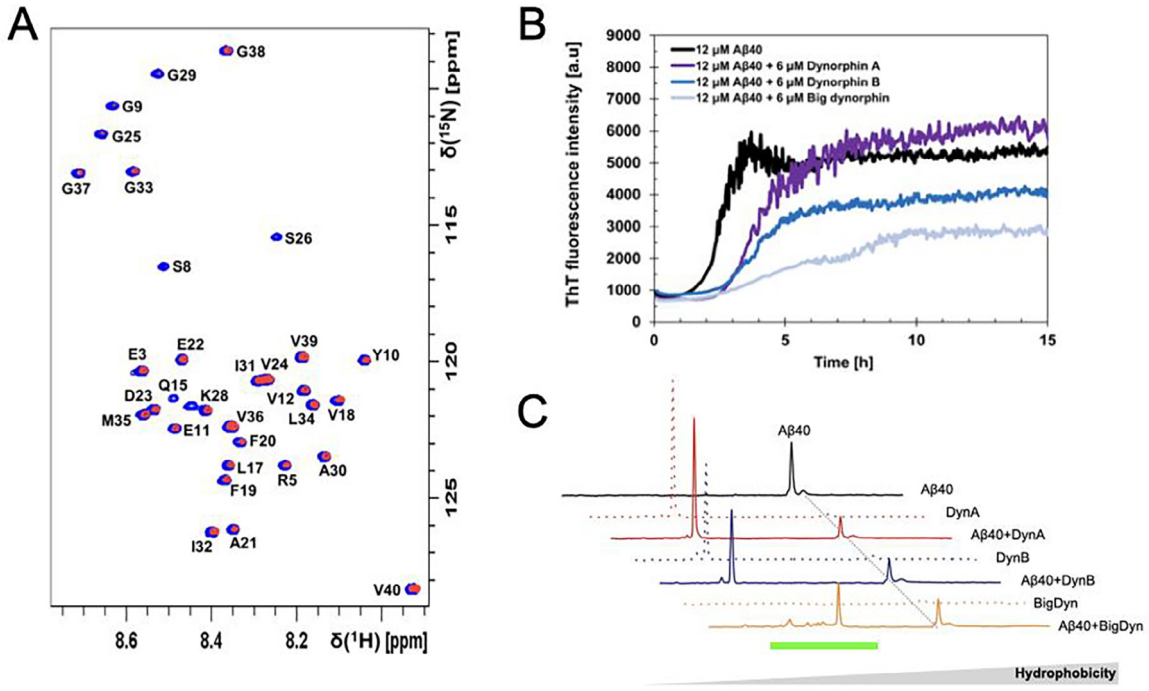

Fig. 2. The dynorphin-Aβ_{40} cross-interaction. A. 2D NMR experiments show Aβ_{40} residue-specific perturbations in the presence of big dynorphin (BigDyn). 700 MHz ^{1}H-^{15}N-HSQC spectra of 84 μM monomeric ^{15}N-labeled Aβ_{40} peptide alone (blue amide crosspeaks) and in the presence of 84 μM BigDyn (red amide crosspeaks) in 10 mM sodium phosphate buffer pH 7.4 at + 5 °C. B. Attenuated Aβ_{40} peptide fibrillation kinetics in the presence of dynorphin peptides. 12 μM monomeric Aβ_{40} peptides were incubated in 10 mM sodium phosphate buffer pH 7.4 and 40 μM ThT at + 37 °C under quiescent conditions in the absence and presence of 6 μM dynorphin A (DynA), dynorphin B (DynB) or BigDyn. In the figure the average for each condition calculated from four replicates are shown. The Aβ_{40} peptide stock solution was prepared by size exclusion chromatography (*SEC*) prior to the ThT sample preparation. C. Reverse Phase high pressure liquid chromatography (RP-HPLC) chromatograms for Aβ_{40} + dynorphins mixtures compared to Aβ_{40} alone (25 μM, solid lines) and dynorphins alone (10 μM; dotted lines) incubated during 30 h. The grey dashed line indicates the position of the Aβ_{40} peak, and the green line the position of the peaks specific for Aβ_{40} + BigDyn mixture. Peptide concentrations were kept at 25 μM Aβ_{40}, 10 μM dynorphin, and the mixtures at 25:10 μM Aβ_{40}:dynorphin.

Table 2
Phenomenological parameters determined from sigmoidal curve fitting of the kinetic traces of amyloid aggregate formation shown in Fig. 2B.

	ThT endpoint fluorescence level[1]	$\tau_{½}$ [h]	r_{max} [h^{-1}]
Aβ_{40}	4600 ± 670	2.5 ± 0.2	3.5 ± 0.9
Aβ_{40} + Dyn A	5500 ± 340	4.4 ± 0.6	1.2 ± 0.3
Aβ_{40} + Dyn B	3000 ± 440	3.9 ± 0.5	1.7 ± 0.8
Aβ_{40} + Big Dyn	2600 ± 310	5.6 ± 1.1	0.5 ± 0.1

[1] End point amplitude intensity in ThT kinetics experiments (Fig. 1B).

complexed with BigDyn the Aβ_{40} cross-interaction process is halted, and the Aβ_{40} secondary structure is stabilized in α-helical secondary structures (Fig. 4B). The peptide-peptide contact is within 89–100 % of the total simulation time (Fig. 4 and Supplementary Table S1) and although the nature of the contacts is diverse, BigDyn residues Arg6, Arg9, Arg19 are prominent in stabilizing not only negatively charged residues such as Glu3 and Glu22 in Aβ_{40} but also aromatic residues, such as Phe4 and Phe20. The BigDyn YGGFL signature present at the *N*-terminus (residues 1 to 5) and in the peptide core (residues 20–24) interact with the 18–26 region in Aβ_{40} (Fig. 4C).

4. Discussion

Based on the hypothesis that highly positive peptides such as dynorphins should be able to interact with negatively charged peptides, such as Aβ_{40} we have combined computational and experimental biophysics methods to determine the nature of the interaction and the Aβ_{40} anti-amyloidogenic potential of dynorphins. Then, we have characterized the cytotoxicity of the complexes to evaluate the potential neuroprotective power of dynorphins against Aβ_{40} damage. It has been previously shown that positively charged endogenous molecules such as polyamines

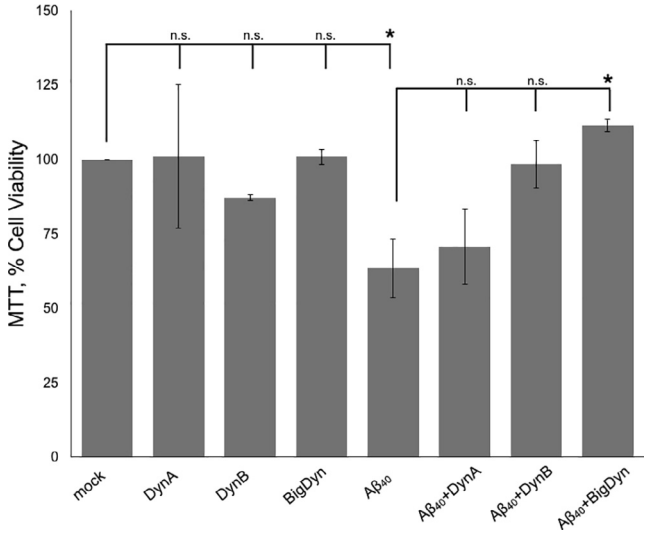

Fig. 3. Amyloid-induced cell toxicity in SH-SY5Y cells. The effect on cell viability of Aβ_{40} aggregates and single dynorphins was compared to buffer alone (mock) is represented as the average of at least three independent experiments ± S.E.M. The effect on cell viability of aggregates derived from Aβ_{40} incubated with dynorphins aggregates (Aβ_{40}:dynorphin; 3.75:1.5 μM) was compared to Aβ_{40} (3.75 μM). Conditions yielding non-significant and significant ($p < 0.05$) differences are indicated by n.s. and *, respectively.

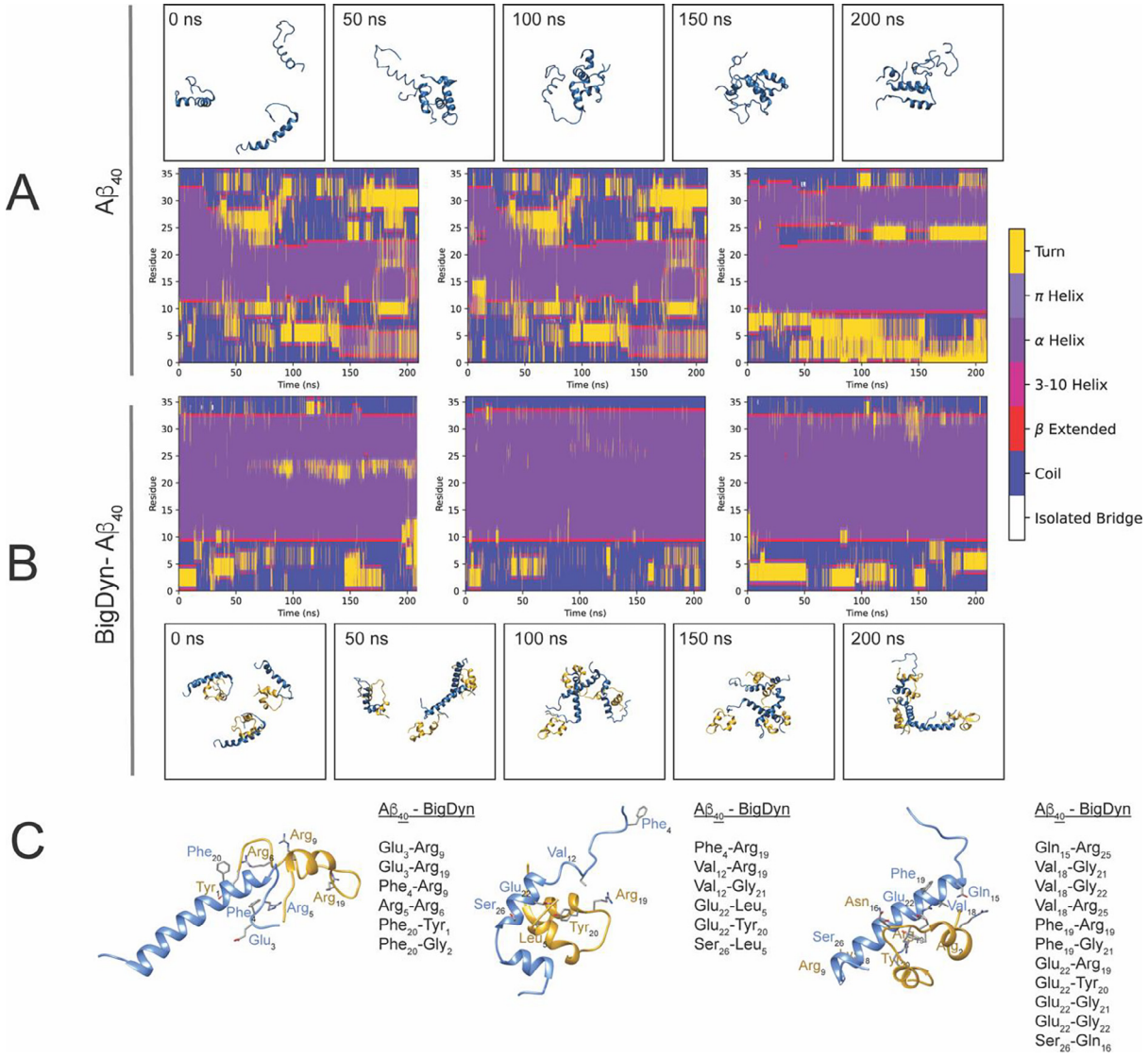

Fig. 4. Aβ40 secondary structure conversions induced by the BigDyn cross-interaction. A. Time specific snapshots of the complex of three $A\beta_{40}$ peptides and their respective secondary structure conversions. B. Time specific snapshots of the complex of three $A\beta_{40}$-BigDyn highlighting only the three $A\beta_{40}$ peptides secondary structure conversions. C. Molecular determinants driving the $A\beta_{40}$-BigDyn cross-interaction (blue and gold, respectively), with a total simulation contact time of 90% (left), 89% (middle), and 100% (right). The residues indicated are the ones in close contact (<5Å) for at least 30% of the simulation time (Supporting Table S1).

and metal ions are able to interfere with Aβ aggregation and toxicity [9,37,38].

Here we have used an *in vitro* biophysical and cellular biology methods to confirm and characterize the physical cross-interaction between endogenous opioid peptides, such as dynorphins, and $A\beta_{40}$ peptides. Our results show that dynorphins cross-interact *in silico* with $A\beta_{40}$. Physico-chemical properties such as charge, electrostatic potential, and hydrophobicity favour the interaction as shown by the global, and interfacial scores in docking results, especially for BigDyn. *In vitro*, dynorphins interact with $A\beta_{40}$ early in the aggregation process as shown by ThT aggregation kinetics and monomeric NMR interaction data for BigDyn. DynA and DynB affect the aggregation kinetics without exerting a significant neuroprotective effect in cell viability experiments. BigDyn prevents and slows down the amyloid aggregation of both monomeric and nucleated $A\beta_{40}$ samples. The aggregates derived from the $A\beta_{40}$ and BigDyn cross-interactions are less hydrophobic, and show a neuroprotective behavior in cell viability assays, compared to $A\beta_{40}$ aggregates alone. The neuroprotective mechanism of BigDyn will require further study, because the recovery of cytotoxicity by BigDyn in Fig. 3 could be due to, among other possibilities, the inhibition of monomer to oligomer formation or the binding to oligomers and the hindering their interaction with the cell surface [39–41], taking into account that BigDyn prevents the aggregation of both monomeric and nucleated $A\beta_{40}$ samples. Among dynorphins, BigDyn appears to be more than the mere combination of DynA and DynB. BigDyn factors such as higher helical content, amphipatic character, size, and positive charge [24] account for a stronger interaction with hydrophobic and negatively charged $A\beta_{40}$. As shown in our MD simulations, $A\beta_{40}$ is prone to aggregate and collapse in water solution. The presence of BigDyn prevents the collapse of $A\beta_{40}$ and the transition to β-strand, stabilizing $A\beta_{40}$ in an α-helical secondary structure through the interaction with hydrophobic residues in the $A\beta_{40}$ disordered *N*-terminus (Phe4, Arg5 and Val12), and the Val18-Phe19-Phe20 hydrophobic core, as shown by short antiamyloid CPP-derived peptides [42]. The 16–22 region of the amyloid peptide has been shown as a key element in the triggering of dimerization process [43]. BigDyn positive residues seem to be key in the interaction with hydrophobic residues, but also with key negatively charged residues in Aβ,

such as Glu3 and Glu22, where the latter is a key residue in AD aggregation kinetics and pathology [44].

BigDyn as an intermediate precursor of DynA, appears as an interesting target to decrease pathological DynA levels [21]. Derived from our results, BigDyn may act as an attenuator of cell toxicity and amyloid aggregation, becoming a potential peptidic therapy in AD, by stabilizing $A\beta_{40}$ aggregation in a less toxic or neuroprotective state. Altogether, our results indicate that $A\beta_{40}$ and dynorphins cross-interactions have potential pathophysiological implications in AD, which are worthy to explore further from the therapeutics and pathology perspectives, such as the basis for the design of inhibitory BigDyn-based peptides as therapeutic tools for the treatment of AD. As both the Aβ and dynorphin peptides are known to interact with membranes [45,46] – Aβ is even produced by enzymatic cleavage of the AβPP (Amyloid-β precursor protein) membrane protein - it appears likely that *in vivo*, the two types of peptides will encounter each other and interact in membrane locations. In the amyloid field, the study of peptide-peptide cross-interactions is key [3,11,12,47,48] to characterize the physiological environment and determine which players can act as pro-amyloid or anti-amyloid agents opening new therapeutic windows in neurodegenerative disorders, such as studies on the cross-interaction between α-synuclein and endogenous peptides used as peptide-therapeutic scaffolds for Parkinson's disease [49].

Funding

This work was supported by the Spanish Ministry of Science and Innovation and Agencia Estatal de Investigación through grant MCIN/AEI/ https://doi.org/10.13039/501100011033 (projects 2019-108434GB-I00 to M.A.-A., PID2020-117691RB-I00 to F.J.M., and PID2020-120222GB-I00 to A.P.-M.), Generalitat Valenciana (project AICO/2020/066 to M.A-A.), FEDER Funds and by the "María de Maeztu Programme" for Units of Excellence in R&D (award CEX2018-000792-M). A.G. was supported by grants from the Swedish Research Council.

CRediT authorship contribution statement

Lucía Gallego-Villarejo: Investigation, Writing – review & editing. **Cecilia Wallin:** Investigation, Writing – review & editing. **Sylwia Król:** Investigation, Writing – review & editing. **Jennifer Enrich-Bengoa:** Investigation, Writing – review & editing. **Albert Suades:** Investigation, Writing – review & editing. **Marcel Aguilella-Arzo:** Investigation, Resources, Writing – review & editing. **María José Gomara:** Resources, Writing – review & editing. **Isabel Haro:** Resources, Writing – review & editing. **Sebastian Wärmlander:** Writing – review & editing. **Francisco J. Muñoz:** Conceptualization, Resources, Writing – review & editing, Funding acquisition. **Astrid Gräslund:** Conceptualization, Resources, Writing – review & editing, Funding acquisition. **Alex Perálvarez-Marín:** Conceptualization, Investigation, Resources, Writing – original draft, Writing – review & editing, Funding acquisition.

Declaration of Competing Interest

The authors declare that they have no known competing financial interests or personal relationships that could have appeared to influence the work reported in this paper.

Acknowledgments

The authors would like to thank Mr. Jordi Pujols Pujol for skillful technical assistance in RP-HPLC experiments, and Mr. Mateo Calle Velásquez for skillful assistance in the docking process.

Appendix A. Supplementary data

Supplementary data to this article can be found online at https://doi.org/10.1016/j.csbj.2022.10.014.

References

[1] Hardy J, Selkoe DJ. The amyloid hypothesis of Alzheimer's disease: progress and problems on the road to therapeutics. Science 2002;297:353–6. https://doi.org/10.1126/science.1072994.
[2] Selkoe DJ, Hardy J. The amyloid hypothesis of Alzheimer's disease at 25 years. EMBO Mol Med 2016;8:595–608. 10.15252/emmm.201606210.
[3] Picón-Pagès P, Bonet J, García-García J, Garcia-Buendia J, Gutierrez D, Valle J, et al. Human albumin impairs amyloid β-peptide fibrillation through its C-terminus: from docking modeling to protection against neurotoxicity in Alzheimer's disease. Comput Struct Biotechnol J 2019;17:963–71. https://doi.org/10.1016/j.csbj.2019.06.017.
[4] Valls-Comamala V, Guivernau B, Bonet J, Puig M, Perálvarez-Marín A, Palomer E, et al. The antigen-binding fragment of human gamma immunoglobulin prevents amyloid β-peptide folding into β-sheet to form oligomers. 2017. 10.18632/oncotarget.17074.
[5] Doig AJ, Del Castillo-Frias MP, Berthoumieu O, Tarus B, Nasica-Labouze J, Sterpone F, et al. Why Is Research on Amyloid-β Failing to Give New Drugs for Alzheimer's Disease? ACS Chem Neurosci 2017;8:1435–7. https://doi.org/10.1021/acschemneuro.7b00188.
[6] Sevigny J, Chiao P, Bussière T, Weinreb PH, Williams L, Maier M, et al. The antibody aducanumab reduces Aβ plaques in Alzheimer's disease. Nature 2016;537:50–6.
[7] Hori Y, Hashimoto T, Nomoto H, Hyman BT, Iwatsubo T. Role of apolipoprotein E in β-amyloidogenesis: Isoform-specific effects on protofibril to fibril conversion of Aβ in vitro and brain Aβ deposition in vivo. J Biol Chem 2015;290:15163–74. https://doi.org/10.1074/jbc.M114.622209.
[8] Gu L, Guo Z. Alzheimer's Aβ42 and Aβ40 peptides form interlaced amyloid fibrils. J Neurochem 2013;126:305–11. https://doi.org/10.1111/jnc.12202.
[9] Warmlander S, Tiiman A, Abelein A, Luo J, Jarvet J, Soderberg KL, et al. Biophysical studies of the amyloid beta-peptide: interactions with metal ions and small molecules. ChemBioChem 2013;14:1692–704. https://doi.org/10.1002/cbic.201300262.
[10] Tamano H, Takeda A. Is interaction of amyloid beta-peptides with metals involved in cognitive activity? Metallomics 2015;7:1205–12. https://doi.org/10.1039/c5mt00076a.
[11] Luo J, Warmlander SKTS, Graslund A, Abrahams JP. Cross-interactions between the Alzheimer disease amyloid-beta peptide and other amyloid proteins: a further aspect of the amyloid cascade hypothesis. J Biol Chem 2016;291:16485–93. https://doi.org/10.1074/jbc.R116.714576.
[12] Valls-Comamala V, Guivernau B, Bonet J, Puig M, Peralvarez-Marin A, Palomer E, et al. The antigen-binding fragment of human gamma immunoglobulin prevents amyloid beta-peptide folding into beta-sheet to form oligomers. Oncotarget 2017;8:41154–65. 10.18632/oncotarget.17074.
[13] Yakovleva T, Bazov I, Cebers G, Marinova Z, Hara Y, Ahmed A, et al. Prodynorphin storage and processing in axon terminals and dendrites. FASEB J Off Publ Fed Am Soc Exp Biol 2006;20:2124–6. https://doi.org/10.1096/fj.06-6174fje.
[14] O'Connor C, White KL, Doncescu N, Didenko T, Roth BL, Czaplicki G, et al. NMR structure and dynamics of the agonist dynorphin peptide bound to the human kappa opioid receptor. Proc Natl Acad Sci U S A 2015;112:11852–7. https://doi.org/10.1073/pnas.1510117112.
[15] Hauser KF, Aldrich JV, Anderson KJ, Bakalkin G, Christie MJ, Hall ED, et al. Pathobiology of dynorphins in trauma and disease. Front Biosci 2005;10:216–35.
[16] Perini DA, Aguilella-Arzo M, Alcaraz A, Perálvarez-Marín A, Queralt-Martín M. Dynorphin A induces membrane permeabilization by formation of proteolipidic pores. Insights from electrophysiology and computational simulations. Comput Struct Biotechnol J 2022;20:230–40. https://doi.org/10.1016/j.csbj.2021.12.021.
[17] Gasteiger E, Hoogland C, Gattiker A, Duvaud S, Wilkins M., Appel R., et al. Protein Identification and Analysis Tools on the ExPASy Server. Proteomics Protoc. Handb., 2005, p. 571–607. 10.1385/1-59259-890-0:571.
[18] Barg J, Belcheva M, Rowinski J, Ho A, Burke WJ, Chung HD, et al. Opioid receptor density changes in Alzheimer amygdala and putamen. Brain Res 1993;632:209–15. https://doi.org/10.1016/0006-8993(93)91155-L.
[19] Mathieu-Kia AM, Fan LQ, Kreek MJ, Simon EJ, Hiller JM. m-, d- and k-opioid receptor populations are differentially altered in distinct areas of postmortem brains of Alzheimer's disease patients. Brain Res 2001;893:121–34. https://doi.org/10.1016/S0006-8993(00)03302-3.
[20] Risser D, You ZB, Cairns N, Herrera-Marschitz M, Seidl R, Schneider C, et al. Endogenous opioids in frontal cortex of patients with Down syndrome. Neurosci Lett 1996;203:111–4. https://doi.org/10.1016/0304-3940(95)12275-3.
[21] Yakovleva T, Marinova Z, Kuzmin A, Seidah NG, Haroutunian V, Terenius L, et al. Dysregulation of dynorphins in Alzheimer disease 2007;28:1700–8. 10.1016/j.neurobiolaging.2006.07.002.

[22] Ménard C, Herzog H, Schwarzer C, Quirion R. Possible role of dynorphins in Alzheimer's disease and age-related cognitive deficits. Neurodegener Dis 2014;13:82–5. https://doi.org/10.1159/000353848.
[23] Wilcox KC, Lacor PN, Pitt J, Klein WL. Aβ oligomer-induced synapse degeneration in Alzheimer's disease. Cell Mol Neurobiol 2011;31:939–48. https://doi.org/10.1007/s10571-011-9691-4.
[24] Hugonin L, Barth A, Gräslund A, Perálvarez-Marín A. Secondary structure transitions and aggregation induced in dynorphin neuropeptides by the detergent sodium dodecyl sulfate. Biochim Biophys Acta – Biomembr 2008;1778:2580–7. https://doi.org/10.1016/j.bbamem.2008.07.011.
[25] Coles M, Bicknell W, Watson AA, Fairlie DP, Craik DJ. Solution Structure of Amyloid β-Peptide(1−40) in a Water−Micelle Environment. Is the Membrane-Spanning Domain Where We Think It Is?,. Biochemistry 1998;37:11064–77. 10.1021/bi972979f.
[26] Schneidman-Duhovny D, Inbar Y, Nussinov R, Wolfson HJ. PatchDock and SymmDock: servers for rigid and symmetric docking. Nucleic Acids Res 2005;33:W363–7. https://doi.org/10.1093/nar/gki481.
[27] Lyskov S, Chou F-C, Conchúir SÓ, Der BS, Drew K, Kuroda D, et al. Serverification of molecular modeling applications: the Rosetta online server that includes everyone (ROSIE). PLoS ONE 2013;8:e63906.
[28] Chaudhury S, Berrondo M, Weitzner BD, Muthu P, Bergman H, Gray JJ. Benchmarking and analysis of protein docking performance in Rosetta v3.2. PLoS ONE 2011;6:e22477.
[29] Wu EL, Cheng X, Jo S, Rui H, Song KC, Dávila-Contreras EM, et al. CHARMM-GUI Membrane Builder toward realistic biological membrane simulations. J Comput Chem 2014. https://doi.org/10.1002/jcc.23702.
[30] Huang J, Rauscher S, Nawrocki G, Ran T, Feig M, De Groot BL, et al. CHARMM36m: An improved force field for folded and intrinsically disordered proteins. Nat Methods 2016;14:71–3. https://doi.org/10.1038/nmeth.4067.
[31] Phillips JC, Braun R, Wang W, Gumbart J, Tajkhorshid E, Villa E, et al. Scalable molecular dynamics with NAMD. vol. 26. 2005. 10.1002/jcc.20289.
[32] Jan A, Hartley DM, Lashuel HA. Preparation and characterization of toxic Abeta aggregates for structural and functional studies in Alzheimer's disease research. Nat Protoc 2010;5:1186–209. https://doi.org/10.1038/nprot.2010.72.
[33] Rodina NP, Sulatsky MI, Sulatskaya AI, Kuznetsova IM, Uversky VN, Turoverov KK. Photophysical properties of fluorescent probe thioflavin T in crowded milieu. J Spectrosc 2017;2017. https://doi.org/10.1155/2017/2365746.
[34] Biancalana M, Koide S. Molecular mechanism of Thioflavin-T binding to amyloid fibrils. Biochim Biophys Acta – Proteins Proteomics 2010. https://doi.org/10.1016/j.bbapap.2010.04.001.
[35] Hellstrand E, Boland B, Walsh DM, Linse S. Amyloid β-protein aggregation produces highly reproducible kinetic data and occurs by a two-phase process. ACS Chem Neurosci 2010;1:13–8. https://doi.org/10.1021/cn900015v.
[36] Danielsson J, Andersson A, Jarvet J, Graslund A. 15N relaxation study of the amyloid beta-peptide: structural propensities and persistence length. Magn Reson Chem 2006;44 Spec No:S114-21. 10.1002/mrc.1814.
[37] Luo J, Yu C-H, Yu H, Borstnar R, Kamerlin SCL, Gräslund A, et al. Cellular polyamines promote amyloid-beta (Aβ) peptide fibrillation and modulate the aggregation pathways. ACS Chem Neurosci 2013;4:454–62. https://doi.org/10.1021/cn300170x.
[38] Luo J, Mohammed I, Wärmländer SKTS, Hiruma Y, Gräslund A, Abrahams JP. Endogenous polyamines reduce the toxicity of soluble Aβ peptide aggregates associated with Alzheimer's disease. Biomacromolecules 2014;15:1985–91. https://doi.org/10.1021/bm401874j.
[39] Santuz H, Nguyen PH, Sterpone F, Derreumaux P. Small oligomers of Aβ42 protein in the bulk solution with AlphaFold2. ACS Chem Neurosci 2022;13:711–3. https://doi.org/10.1021/acschemneuro.2c00122.
[40] Nguyen PH, Ramamoorthy A, Sahoo BR, Zheng J, Faller P, Straub JE, et al. Amyloid oligomers: a joint experimental/computational perspective on Alzheimer's disease, Parkinson's disease, Type II diabetes, and amyotrophic lateral sclerosis. Chem Rev 2021;121:2545–647. https://doi.org/10.1021/acs.chemrev.0c01122.
[41] Nguyen HL, Linh HQ, Matteini P, La Penna G, Li MS. Emergence of barrel motif in amyloid-β trimer: a computational study. J Phys Chem B 2020;124:10617–31. https://doi.org/10.1021/acs.jpcb.0c05508.
[42] Henning-Knechtel A, Kumar S, Wallin C, Król S, Wärmländer SKTS, Jarvet J, et al. Designed cell-penetrating peptide inhibitors of amyloid-beta aggregation and cytotoxicity. Cell Reports Phys Sci 2020;1:. https://doi.org/10.1016/j.xcrp.2020.100014100014.
[43] Man VH, He X, Derreumaux P, Ji B, Xie X-Q, Nguyen PH, et al. Effects of all-atom molecular mechanics force fields on amyloid peptide assembly: the case of Aβ (16–22) dimer. J Chem Theory Comput 2019;15:1440–52. https://doi.org/10.1021/acs.jctc.8b01107.
[44] Perálvarez-Marín A, Mateos L, Zhang C, Singh S, Cedazo-Mínguez Á, Visa N, et al. Influence of residue 22 on the folding, aggregation profile, and toxicity of the Alzheimer's amyloid β peptide. Biophys J 2009;97:277–85. https://doi.org/10.1016/j.bpj.2009.04.017.
[45] Madani F, Taqi MM, Wärmländer SKTS, Verbeek DS, Bakalkin G, Gräslund A. Perturbations of model membranes induced by pathogenic dynorphin a mutants causing neurodegeneration in human brain. Biochem Biophys Res Commun 2011;411:111–4. https://doi.org/10.1016/j.bbrc.2011.06.105.
[46] Österlund N, Luo J, Wärmländer SKTS, Gräslund A. Membrane-mimetic systems for biophysical studies of the amyloid-β peptide. Biochim Biophys Acta Proteins Proteomics 2019;1867:492–501. https://doi.org/10.1016/j.bbapap.2018.11.005.
[47] Österlund N, Wärmländer SKTS, Gräslund A. Cell-penetrating peptides with unexpected anti-amyloid properties. Pharmaceutics 2022;14. https://doi.org/10.3390/pharmaceutics14040823.
[48] Löhr T, Kohlhoff K, Heller GT, Camilloni C, Vendruscolo M. A small molecule stabilizes the disordered native state of the Alzheimer's Aβ peptide. ACS Chem Neurosci 2022;13:1738–45. https://doi.org/10.1021/acschemneuro.2c00116.
[49] Santos J, Gracia P, Navarro S, Peña-Díaz S, Pujols J, Cremades N, et al. α-Helical peptidic scaffolds to target α-synuclein toxic species with nanomolar affinity. Nat Commun 2021;12:3752. https://doi.org/10.1038/s41467-021-24039-2.